THESIS FOR THE DEGREE OF DOCTOR OF PHILOSOPHY

Statistical methods in single particle fluorescence microscopy

Magnus Röding

Division of Mathematical Statistics
Department of Mathematical Sciences
Chalmers University of Technology and University of Gothenburg
Göteborg, Sweden 2013

Statistical methods in single particle fluorescence microscopy
Magnus Röding
ISBN 978-91-7385-855-7

Doktorsavhandlingar vid Chalmers Tekniska Högskola
Ny serie nr 3536
ISSN 0346-718x

Division of Mathematical Statistics
Department of Mathematical Sciences
Chalmers University of Technology and University of Gothenburg
SE-412 96 Göteborg
Sweden
Telephone +46 (0)31 772 1000

Typeset with LaTeX.
Printed in Göteborg, Sweden 2013

Abstract

The aim of this thesis is stochastic modeling and statistical inference in single particle fluorescence microscopy related to the experimental observation of randomly moving particles.

A central theme is the use of single particle microscopy for estimation of absolute concentration of nanoparticles performing Brownian motion. In Papers I and II, the monodisperse case, i.e. one single diffusion coefficient, is considered. The key idea is to estimate the absolute concentration by first estimating the size of the three-dimensional detection region in which particles are observed. In earlier works, this has been estimated in separate calibration experiments. In Paper I, the detection region size is estimated by modeling the distribution of trajectory lengths (durations) as a function of the size. In Paper II, an alternative method is suggested by studying transition probabilities in a time series of particle counts known as a Smoluchowski process. It is demonstrated that both methods provide very good agreement with reference values and with each other. Paper III is partly based on Paper I, generalizing the results to the polydisperse case, i.e. with a distribution of diffusion coefficients. It is shown that the distribution of diffusion coefficients as well as the total absolute concentration can be satisfactorily estimated.

One crucial step in single particle microscopy is the correct classification of particles and noise in microscope images, since both false negatives and false positives can have a substantial impact on all further analysis. Typically, a plausible set of particles is obtained from a larger set of candidate particles by filtering using manually selected threshold values for intensity, size, shape, and other parameters. In Paper IV, a novel method for automatic selection of such threshold values is introduced, based on an analysis of the correlation structure of a Smoluchowski process distorted by false negatives and false positives. The method shows promise and provides a new paradigm in automated image analysis for single particle microscopy.

Keywords: absolute number concentration, Brownian motion, diffusion, fluorescence microscopy, image analysis, image processing, nanoparticle characterization, particle tracking, Smoluchowski process

Sammanfattning

Syftet med denna avhandling är stokastisk modellering och statistisk slutledning inom så kallad single particle fluorescence microscopy, relaterat till experimentella observationer av partiklar i slumpmässig rörelse.

Ett centralt tema är att använda single particle microscopy for att skatta absolut koncentration av nanopartiklar som utför Brownsk rörelse. I Artikel I och II behandlas det monodispersiva fallet, det vill säga där alla diffusionskoefficienter är lika. Huvudidén är att skatta den absoluta koncentrationen genom att först skatta storleken på den tredimensionella detektionsregionen i vilken partiklar observeras. I tidigare arbeten har denna skattats genom separata kalibreringsexperiment. I Artikel I görs detta genom att modellera distributionen av längder (varaktighet) för trajektorierna som funktion av storleken. I Artikel II föreslås en alternativ metod genom att studera övergångssannolikheter i en tidsserie av partikelantal känd som en Smoluchowskiprocess. Bägge metoderna ger mycket god överensstämmelse med referensvärden och med varandra. Artikel III är delvis baserad på Artikel I och innehåller en generalisering till det polydispersiva fallet när diffusionskoefficienterna följer en fördelning. Fördelningen av diffusionskoefficienter såväl som den totala absoluta koncentrationen kan skattas tillfredsställande bra.

Ett viktigt steg i single particle microscopy är att korrekt klassificera partiklar och brus i mikroskopbilder eftersom både falska negativa och falska positiva kan ha väsentlig påverkan på all efterföljande analys. Vanligt är att en rimlig uppsättning partiklar fås från en större uppsättning kandidatpartiklar genom filtrering med hjälp av manuellt valda tröskelvärden för intensitet, storlek, form och andra parametrar. I Artikel IV introduceras en ny metod för automatiskt val av sådana tröskelvärden, baserat på en analys av korrelationsstrukturen i en Smoluchowskiprocess som "störts" av falska negativa och falska positiva. Metoden ger lovande resultat och ger upphov till en ny paradigm inom automatiserad bildanalys för single particle microscopy.

Nyckelord: absolut antalskoncentration, bildanalys, bildbehandling, Brownsk rörelse, diffusion, fluorescensmikroskopi, karaktärisering av nanopartiklar, particle tracking, Smoluchowskiprocess

Acknowledgements

I would like to thank my advisors Mats Rudemo and Aila Särkkä for invaluable contributions and support during this work.

Supramolecular Biomaterials (SuMo) is acknowledged for providing a stimulating inter-disciplinary network of people, through which I have found almost all of my collaborations.

I would also like to acknowledge many other people with whom I have collaborated:

First of all, my main co-workers Kevin Braeckmans and Hendrik Deschout, as well as Thomas Martens, Eliza Zagato, and a number of other people at the Laboratory of General Biochemistry and Physical Pharmacy and the Center for Nano- and Biophotonics at Ghent University, Ghent, Belgium.

Also, Ming Guo and David Weitz in the Experimental Soft Condensed Matter Group at the School of Engineering and Applied Sciences and the Department of Physics at Harvard University, Cambridge, Massachusetts, USA.

Last but not least, all the people here in Sweden with whom I have worked and discussed in the Department of Mathematical Sciences at Chalmers, the Applied Surface Chemistry group at the Department of Chemical and Biological Engineering at Chalmers, the Swedish NMR Center in the Hasselblad Laboratory at Gothenburg University, the Swedish Institute for Food and Biochemistry (SIK), the Physical Chemistry group at the Department of Chemistry at Lund University, and the Supramolecular Biomaterials (SuMo) group. There are too many people to make a comprehensive list, but Diana Bernin, Jenny Jonasson, Niklas Lorén, Magnus Nydén, and Kristin Sott deserve to be mentioned. So does, on the other hand, quite a few more people.

Anders Jonsson is acknowledged for proofreading this thesis.

I also extend my thanks to current and former colleagues both in and outside the Department of Mathematical Sciences for a fruitful working environment and help with small matters as well as not so small ones. A list of you all would be way too long.

Gothenburg, April 2013

Magnus Röding

List of papers

This thesis includes the following papers.

I. **M. Röding**, H. Deschout, K. Braeckmans, and M. Rudemo (2011). Measuring absolute number concentrations of nanoparticles using single-particle tracking. *Physical Review E*, 84, 031920.

II. **M. Röding**, H. Deschout, K. Braeckmans, and M. Rudemo (2013). Measuring absolute nanoparticle number concentrations from particle count time series. *To appear in Journal of Microscopy.*

III. **M. Röding**, H. Deschout, K. Braeckmans, A. Särkkä, and M. Rudemo (2013). Self-calibrated concentration measurements of polydisperse nanoparticles. *Submitted.*

IV. **M. Röding**, H. Deschout, K. Braeckmans, A. Särkkä, and M. Rudemo (2013). Automatic particle detection in microscopy using temporal correlations. *Submitted.*

The contribution of the author of this thesis was for all Papers I through IV the majority of the writing and the derivations, algorithm development, implementation, simulation studies, and application to experimental data.

List of papers not included in this thesis

B. Naeye, H. Deschout, **M. Röding**, M. Rudemo, J. Delanghe, K. Devreese, J. Demeester, K. Braeckmans, S. C. de Smedt, and K. Raemdonck (2011). Hemocompatibility of siRNA loaded dextran nanogels. *Biomaterials*, 32, 9120-9127.

M. Röding, D. Bernin, J. Jonasson, A. Särkkä, D. Topgaard, M. Rudemo, and M. Nydén (2012). The gamma distribution model for pulsed-field gradient NMR studies of molecular-weight distributions of polymers. *Journal of Magnetic Resonance*, 222, 105-111.

M. Nordin, C. Abrahamsson, C. Hamngren Blomqvist, **M. Röding**, E. Olsson, M. Nydén, and M. Rudemo (2013). Estimation of mass thickness response of aggregated silica nanospheres from high angle annular dark-field scanning transmission electron micrographs. *Submitted*.

M. Röding, M. Guo, D. Weitz, M. Rudemo and A. Särkkä (2013). Identifying directional persistence in intracellular particle motion using Hidden Markov Models. *Submitted*.

H. Deschout, K. Raemdonck, S. Stremersch, P. Maoddi, G. Mernier, P. Renaud, S. Jiguet, A. Hendrix, M. Bracke, R. Van den Broecke, **M. Röding**, M. Rudemo, J. Demeester, S. C. De Smedt, K. Neyts, and K. Braeckmans (2013). Disposable microfluidic chip with integrated light sheet illumination enables size and concentration measurements of submicron membrane vesicles in biofluids for diagnostics. *Submitted*.

No particles were harmed in the making of this thesis.

In God we trust, all others bring data.

- William Edwards Deming (1900 - 1993)

Contents

Chapter 1

Introduction

The purpose of this chapter is to act as an introduction to the field and to cover the key parts of the included papers, providing a reference and starting point for reading these. We shall cover the basics of single particle microscopy, particle detection and tracking, and concentration measurements with an emphasis on areas directly related to the papers included in this thesis. This thesis is in part an adaptation of the author's licentiate thesis Röding (2011).

1.1 Single particle microscopy

With several significant scientific advances, e.g. highly sensitive camera sensors, high-quality optics and lasers, improved fluorescence labeling of particles, and increased computer power for image analysis, single particle and single particle tracking techniques have emerged as cornerstone technology. These techniques are used more and more in such fields as biological physics, nanophysics, biochemistry, cell biology, and pharmacy, with a steadily increasing number of publications each year. This reflects the needs for a deeper understanding of physical and biological mechanisms and characterization of nanoparticulate matter for use e.g. in drug delivery, in biomedical imaging, and as biomarkers, see Remaut et al. (2007), Nune et al. (2009), Chironi et al. (2009), Doevre et al. (2009), Deniz et al. (2008), Nel et al. (2009), Soenen et al. (2009), Lundqvist et al. (2008), Gaumet et al. (2008), Koide et al. (2008), Decuzzi et al. (2010), Morris et al. (2009), Vysotskii et al. (2009), van Gaal et al. (2009), and

Montes-Burgos et al. (2010). The most obvious strengths of the techniques are that spatial and temporal resolution can be very high, that individual particle behavior can be resolved instead of only ensemble averages, and that the advantages over some other techniques when performing studies in undiluted biological fluids are substantial (Braeckmans et al., 2010a; Saxton, 2009; Levi and Gratton, 2010; Kelley et al., 2001).

The typical single particle microscope setup is a wide-field or confocal fluorescence microscope, with the sample being illuminated by laser light, since control over the emission wavelength allows for efficient excitation of fluorescent dyes. The images are captured either by a CCD camera (widefield), when illuminating the whole sample at once, or by collecting photons locally (confocal laser scanning), focusing the illumination into a moving diffraction-limited spot (Braeckmans et al., 2010b; Levi and Gratton, 2010; Zlatanova and van Holde, 2006). The type of particles to be observed depends on the application, but typically either fluorescently labeled man-made macromolecules like polystyrene nanospheres (Braeckmans et al., 2010a; Deniz et al., 2008), fluorescent semiconductor nanocrystals (quantum dots) (Lim et al., 2003; Frangioni, 2006), or actual biological macromolecules with a single fluorescent dye molecule attached to a specific location (Zlatanova and van Holde, 2006; Braeckmans et al., 2010a) are used.

The rôle of microscopy and scientific imaging as a whole is gradually moving more and more from qualitative to quantitative. Mere observation is replaced by measurement and the reduction of data into meaningful and interpretable form whenever possible. It is easier than ever to extract information from image data with the computing resources of today. On the other hand, with increasingly complex studies comes the need for reliability, consistency, and repeatability, not the least for potential diagnostic tools and clinical applications. The situation is perhaps reminiscent of that of some fields in bioinformatics: the amount of data that can be acquired is endless, but to extract meaningful information is a daunting task.

This thesis is a contribution to turning microscopy into this more quantitative paradigm.

1.2 Detection and tracking

The first steps of image analysis for particle detection and tracking are usually unsharp filtering, background subtraction, and other similar steps (Braeckmans et al., 2010b), although the exact implementation can differ greatly between

investigations. Provided (i) that the particles are sufficiently far apart (with the distance measured in the focal plane, perpendicular to the optical axis) so that the distance between them exceeds the diffraction limit and (ii) that the particles are so small (less than ∼200 nm, depending somewhat on wavelength) so that it is impossible to optically resolve them in the visible light spectrum according to Abbe's law (Walter et al., 2008), the particles will appear as Gaussian-like intensity distributions, so called diffraction-limited spots. There are many reasons why actual intensity profiles for particles deviate from this ideal distribution, e.g. large deviations from the focal plane, large particle sizes, un-even illumination, and one particle being occluded by another. In any case, it is not the particle *per se* that is imaged in fluorescence microscopy, but rather the intensity distribution of the photon emission from the fluorescent molecules convolved with a (Gaussian-like) Airy disk point spread function with a Full Width at Half Maximum depending on the emission wavelength and the numerical aperture (Holtzer and Schmidt, 2010; Saxton and Jacobson, 1997).

After initial image analysis, the next step is the actual particle detection. How to do this is all but standardized. There are many different software solutions and algorithms out there and many investigators write their own code. As a result, the particle detection can differ substantially between different studies. The obvious difficulty is how to systematically discriminate between particles and noise. Some authors perform particle detection prior to and independently of particle tracking. Others have made attempts to completely integrate the particle detection and particle tracking phases, making use of prior information from previous particle positions to produce a more reliable particle detection and tracking altogether (Sage et al., 2005; Jaqaman et al., 2008; Smal et al., 2008; Meijering et al., 2009). Particle detection can be a tricky business, especially in the context of living cells, where the same particle can change its appearance over time and complex biological structures can be visible and thus interfere with the signal of interest (Toomre et al., 1999).

Regardless of the method, there will always be ambiguities as to how bright and how large a particle candidate should be in order to be accepted as a particle, and any automatic method will make at least some choices that would appear counter-intuitive for a human operator. There are many particle tracking studies, even relatively recent, which were performed by manually picking out a few apparently interesting particles which are then manually tracked (McDonald et al., 2002). However, the manual workload and the subjectivity makes manual tracking quite unattractive (Zimmer et al., 2002).

We shall consider only particle detection performed independently of particle tracking. Detection of candidate particles can be performed in a variety of ways,

e.g. simple thresholding (global or local) or wavelet decomposition and filtering (Genovesio et al., 2006; Smal et al., 2010; Bornfleth et al., 1998; Braeckmans et al., 2010b; Thomann et al., 2002). One common approach is to accept only a subset of the candidate particles as actual particles by thresholding based on parameters such as intensity, size, shape, and contrast (Braeckmans et al., 2010a,b). Some ambiguities can be resolved by using a very diluted sample and removing particle candidates that appear not to be part of a (sufficiently long) trajectory, which is also beneficial since it simplifies the tracking phase (Crocker and Grier, 1996; Apgar et al., 2000; Jaqaman et al., 2008).

After (or in conjunction with) particle detection, localization and linking (tracking) is performed, but we shall not be overly concerned with the details. We refer the reader to Cheezum et al. (2001) and Carter et al. (2005) for particle localization methods by centroid or least squares fitting and to Yildiz and Selvin (2004), Bausch and Weitz (2002), Thompson et al. (2002), Ober et al. (2004), Mortensen et al. (2010), and Deschout et al. (2012) for localization accuracy and precision.

1.3 Smoluchowski processes and particle detection

At the same time as the groundbreaking theories of Brownian motion were suggested by A. Einstein (Einstein, 1905), several authors made parallell investigations. One of the most prominent is M. von Smoluchowski, who provided new theories of Brownian motion and of the inherently probabilistic nature of thermodynamics at the microscopic scale by studying what he called fluctuations of concentration, or fluctuations of particle counts, in a small volume element (von Smoluchowski, 1906, 1916). His studies were confirmed experimentally, e.g. by Svedberg and Inouye (1911) and Westgren (1916). Time series of particle counts are in this context called Smoluchowski processes, whether the generating motion is Brownian motion or any other motion. In this chapter, we will discuss Smoluchowski processes and their somewhat unexpected use as a means of particle detection in image analysis for single particle microscopy.

Consider a small volume element ω in which particles can be observed and counted, i.e. a detection region. The volume element is centered in a much larger (infinite) volume Ω, i.e. a liquid suspension. It makes sense to think of Ω as $\mathbf{R}^d$. Suppose now that Ω contains a large number of particles in diffusion equilibrium i.e. uniformly distributed and subject to some random forces (marginally, the particles can be thought of as distributed according to a homogeneous Poisson point process). A random number of particles are then moving in and out of ω. The (stationary) Smoluchowski process is then the number of

particles in ω at times $0, \Delta t, 2\Delta t, ...$, denoted by $X(0), X(\Delta t), X(2\Delta t), ...$ for some time lag Δt. If $\Omega = \mathbf{R}^d$, the distribution of $X(n\Delta t)$ is Poisson for every n (Chandrasekhar, 1943) (particles described by a homogeneous Poisson point process maintain the same marginal property indefinitely (Doob, 1953; Daley and Vere-Jones, 2003)). Let the mean and variance of the process both be μ. This process is in principle encountered in single particle microscopy experiments. The main difference between theory and experiment is the occurrence of false negatives and false positives due to ambiguities in particle detection. Henceforth, the observed particle counts are not the same as the true particle counts since they are 'hidden' in the noise. Noise, clutter, diffraction rings, and background and foreground structures will be falsely accepted and identified as particles to some extent (false positives), and particles will be falsely rejected to some extent (false negatives). Both these effects will distort the true Smoluchowski process. The specifics of the image analysis algorithm, e.g. threshold values for intensity, size, shape, and other parameters determine the occurrence of false negatives and false positives.

The correlation function for the Smoluchowski process,

$$R(m) = \frac{E[X(t)X(t+m\Delta t)] - \mu^2}{\mu} \tag{1.1}$$

for $m = 1, 2, ...$ is of particular interest, since it turns out that the correlation for every time lag $m\Delta t$ is affected by the occurrence of false negatives and false positives. Assume that $R(1) = \rho$. It is intuitively clear that the correlation will decrease as an effect of more or less random additions and subtractions of particles. We will quantify this in a simple model.

Introduce for simplicity the notation $X(n\Delta t) = X_n$. Assume that all true particles have the same probability of being falsely identified as noise, independent of all other particles both in the same frame and in other frames. Thus, the number of false negatives in a frame with $X_n = i$ true particles is binomial distributed with index i and parameter ν_- (binomial thinning). Second, assume that the number of false positives is Poisson distributed with parameter ν_+, independent of the number of false positives in other frames and independent of the number of true particles in all frames. Third, assume that false positives and false negatives are independent of each other. Note that false positives and false negatives can occur simultaneously. Consider the process values X_n and X_{n+1}. Assume that they are distorted, i.e.

$$\tilde{X}_n = X_n - T_n + G_n \tag{1.2}$$

and

$$\tilde{X}_{n+1} = X_{n+1} - T_{n+1} + G_{n+1}, \tag{1.3}$$

where T_n and T_{n+1} are the numbers of false negatives and G_n and G_{n+1} are the numbers of false positives in frames n and $n+1$. It can easily be shown that the distorted process is still Poisson, and the analysis in Paper IV gives that the correlation is

$$\tilde{\rho} = \frac{(1-\nu_-)^2\mu}{(1-\nu_-)\mu + \nu_+}\rho \tag{1.4}$$

i.e. a decreasing function of ν_- and ν_+.

Suppose that we are interested in selecting a lower threshold τ for a single parameter A, $0 \leq A < \infty$, may it be intensity, size, or anything else, such that only particles for which $A \geq \tau$ are included in further analysis, and the rest are excluded. Assume that the values of A for true particles are distributed according to a probability density f_{true}, and that the values of A for false particles are distributed according to a probability density f_{false}. Then the parameters describing the occurrence of false negatives and false positives can be expressed as functions of the threshold τ by

$$\nu_- = \int_0^\tau f_{\text{true}}(z)dz \tag{1.5}$$

and

$$\nu_+ = \nu_+^{\max} \int_\tau^\infty f_{\text{false}}(z)dz, \tag{1.6}$$

where $\nu_+^{\max}$ is the maximum expected number (Poisson intensity) of false positives per frame (reached if $\tau = 0$). Typically, the supports of f_{true} and f_{false} are not disjoint, i.e. some amount of false positives and/or false negatives is inevitable.

We note that since

$$\text{sensitivity} = \frac{\text{number of true positives}}{\text{number of true positives} + \text{number of false negatives}} \tag{1.7}$$

and

$$\text{specificity} = \frac{\text{number of true negatives}}{\text{number of true negatives} + \text{number of false positives}}, \tag{1.8}$$

the correlation can alternatively be written as

$$\tilde{\rho} = \frac{\text{sensitivity}^2 \times \mu}{\text{sensitivity} \times \mu + \nu_+^{\max} \times (1 - \text{specificity})}\rho. \tag{1.9}$$

Maximization of the correlation is thus equivalent to minimization of the number of false negatives and false positives in a certain sense, and can be thought

of as an unsupervised binary classification problem with a "loss function" indirectly described by Eq. (1.4) and Eq. (1.9). In Fig. 1.1, examples of Smoluchowski processes extracted using manual and automatic threshold selection are shown. In Fig. 1.2, examples of the effect of different threshold selections on a single sample image are shown.

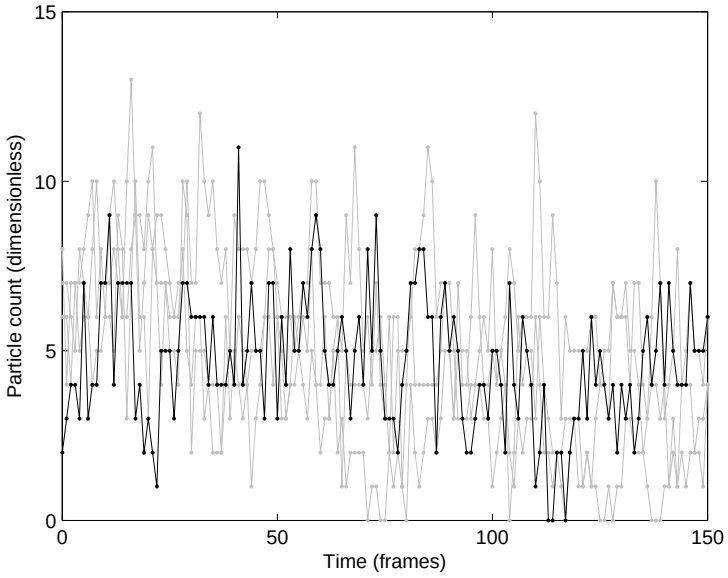

Figure 1.1: Examples of Smoluchowski processes from liposomes diffusing in blood. The results of three independent manual selections (all grey) is very similar to the result of the automatic selection (black).

1.4 Concentration of monodisperse particles

Estimating absolute concentration of diffusing nanoparticles in biological fluids is important in for example nanomedicine and drug delivery for dosage measurements (Braeckmans et al., 2010a; van Gaal et al., 2010; Filipe et al., 2012a,b), for developing nanoparticles for use as contrast agents (Michalet et al., 2005; Delehanty et al., 2009; Welsher et al., 2009; Hong et al., 2012), and for use as diagnostic markers for diseases (Dragovic et al., 2011; Chironi et al., 2009; Doevre

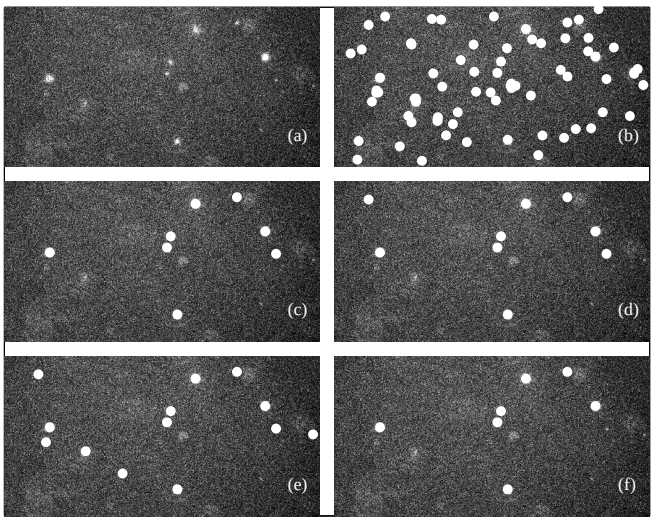

Figure 1.2: Example of the effect of thresholding in a single image in a data set from diffusing liposomes in blood, (a) original image, (b) all candidate particles, (c)-(e) manual selections by three different operators, and (f) automatic selection by the proposed method.

et al., 2009; Khare and Dokholyan, 2007). The crucial step in a concentration measurement using fluorescence microscopy is the estimation (calibration) of the size of the detection region in which particles are detected (and tracked). This size can be estimated in a separate calibration experiment using reference particles as suggested in e.g. Du et al. (2010). However, since particle brightness as well as the image analysis implementation determines the effective size, this procedure is error-prone. In this thesis, two different methods for estimation of the detection region size are proposed.

The experimental setting is the same as that described in the previous section. In a large liquid suspension, particles are diffusing freely and independently of the other particles. In a small detection region, particles are detected (and tracked). The particles are performing Brownian motion with some diffusion coefficient D, characterized by the so called *mean squared displacement*

$$\mathrm{E}[\|X(t) - X(0)\|^2] = 2\mathcal{N}Dt \tag{1.10}$$

which describes the evolution of diffusive motion in $\mathcal{N}$ dimensions (Berg, 1993), where $\mathcal{N} = 3$ for particles moving in space, although we typically observe data only for $\mathcal{N} = 2$. The detection region is modeled as a rectangular box, bounded in the focal plane by the field of view which is determined by the magnification of the microscope and hence known by means of a calibration grid. The axial dimension is estimated using different stochastic models. The collected data constitute one or several time-lapse video sequences with sampling interval Δt between consecutive frames with detected and localized particles.

Using the first method suggested in this thesis, identified particle positions are linked so that trajectories are formed, from which diffusion coefficients can be estimated. The core idea is to model the probability distribution of trajectory lengths (durations) as a function of diffusion coefficient and axial size of the detection region, see Fig. 1.3. The smaller the detection region, the shorter the

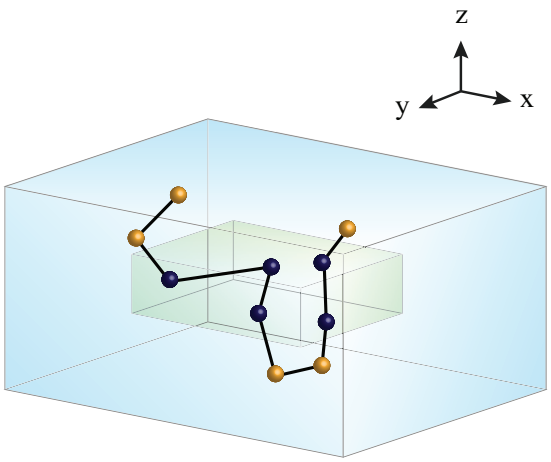

Figure 1.3: Example of particle trajectories. In this example, we see that a single particle gives rise to one trajectory of length 3 positions and one trajectory of length 2 positions.

trajectories are on average. The smaller the diffusion coefficient, the longer the trajectories are on average. Assume that a particle is observed at K equidistant time points (observed in K consecutive frames of a time-lapse video sequence) and then exits the detection region. The same particle may very well enter the detection region again and will then give rise to more than one trajectory. The K positions, denoted by $r_1, r_2, ..., r_K$, can be written as $r_i = r_{i-1} + \Delta G$ for $i = 2, ..., K$, where ΔG is an $\mathcal{N}$-dimensional vector of normally distributed independent components, each with mean zero and variance $2D\Delta t$. We refer to

K as the trajectory length. A simplifying assumption is that particles enter and exit the detection region only by (axial) diffusion, parallel to the optical axis (in the z-direction), which reduces the computational burden substantially. The three-dimensional (3D) system is hence replaced by a one-dimensional (1D) model. Assume that particles diffuse within the suspension $[-A, A]$ and are detected when inside the detection region $[-a, a]$. By using a 1D Gaussian random walk model with increments of mean zero and variance $2D\Delta t$ to describe the particle motion, a numerical approximation by Gaussian basis functions can be used to numerically solve a discrete-time diffusion equation describing the motion of particles entering and exiting the detection region by convolution with a Gaussian diffusion kernel. The details of this approach are described in Paper I and shall not be repeated here. This leads to a numerical scheme for calculation of the probabilities $P_a(K = k)$ for observing different trajectory lengths. Assuming that the observed ensemble of particles is monodisperse, i.e. that all particles share a common diffusion coefficient, and that this diffusion coefficient is known (or estimated by maximum likelihood), we can construct a maximum likelihood estimate $\hat{a}$ of a by fitting the trajectory length distribution to experimental data. Suppose we have observed trajectories with lengths $k \geq k_{\min}$ (it is common to exclude very short trajectories from any analysis due to them being prone to contain false positives (Jaqaman et al., 2008)), and let the number of observed trajectories of length k be N_k. The log-likelihood function $l(a) = l(a; A, \Delta t, D, \{N_k\})$ from which a can be estimated is

$$l(a) = \sum_{k \geq k_{\min}} N_k \log P_a(K = k | K \geq k_{\min}). \tag{1.11}$$

See Fig. 1.4 for an example of a trajectory length distribution. Once having estimated the axial size of the detection region, the number concentration is estimated by dividing the average number of particle positions per frame with the volume of the detection region.

Using the second method proposed in this thesis, identified particles are counted in each frame to form a stochastic process known as a Smoluchowski process. Given a known diffusion coefficient, the transition probabilities of a Markov chain approximation to the process can be used to estimate the axial size of the detection region which is unknown. Assume that we acquire discrete observations of a Smoluchowski process $X(t)$ (a series of particle counts as a function of time) in diffusion equilibrium at regular time intervals with time lapse Δt. Denote the n:th observation by X_n. From one observation to the next, a random number of particles have entered and a random number of particles have left the detection region. Thus

$$X_{n+1} = X_n - O_n + I_n, \tag{1.12}$$

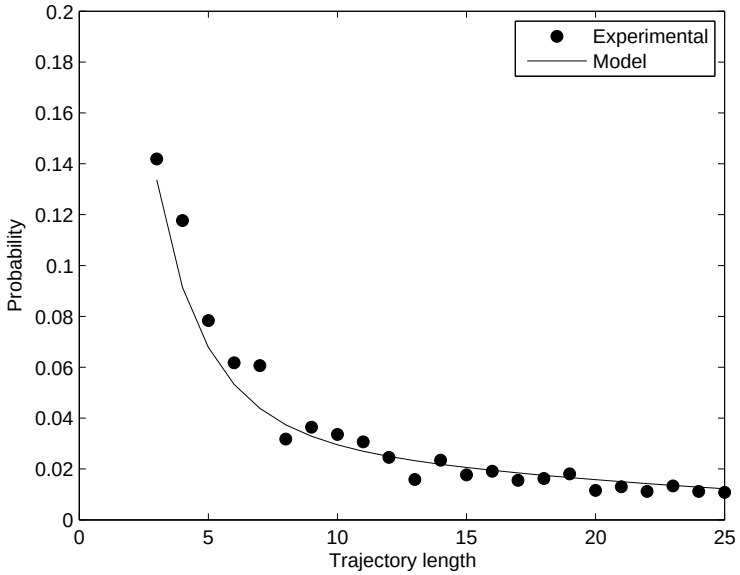

Figure 1.4: Experimental trajectory length distribution from 100 nm nanospheres diffusing in 48 % sucrose solution and the fitted model. The lateral size of the detection region was 34 × 34 μm, and the axial size was estimated to be 1.08 μm. The diffusion coefficient of the particles was 0.54 μm^2.

where O_n is the number of particles (out of the X_n particles initially present) exiting the detection region between the observations X_n and X_{n+1}, and I_n is the number of particles entering the detection region between these observations. Without any additional prior knowledge, a reasonable assumption is that the X_n particles in frame n are uniformly distributed within the detection region. Hence, given $X_n = i$, O_n follows a binomial distribution with index i and parameter μ. Furthermore, we assume that I_n follows a Poisson distribution with parameter λ. The Smoluchowski process is not a Markov process, but it is practical to use a Markov approximation under which transition probabilities (which are *marginally* exact) $p_{ij} = P(X_{n+1} = j|X_n = i)$,$i \geq 0$ and $j \geq 0$, can be found directly using the properties of the Poisson and binomial distributions. Considering a realization $x_1, ..., x_N$, an approximate log-likelihood function $l(\lambda, \mu) = l(\lambda, \mu|x_1, ..., x_N)$ can be obtained. Since μ equals the probability $P_{\text{exit}}(a_z)$ that a uniformly distributed particle exits the detection region we can obtain an estimate $\hat{a}_z$ of the axial size of the detection region by solving

$P_{\text{exit}}(a_z) = \mu$ for a_z. To estimate the number concentration C, we divide the mean number of detected particles per frame by the estimated volume of the detection region. Since the stationary distribution is Poisson with intensity λ/μ, the mean number of detected particles can be estimated by $\hat{\lambda}/\hat{\mu}$. Even though the process is not Markov, the transition probabilities derived are 'marginally' true, i.e. the expression for $P(X_k = x_k|X_{k-1} = x_{k-1})$ is exact for any k (but the full likelihood still underestimates correlations on longer scales than Δt because of the Markov assumption).

1.5 Distributions of diffusion coefficients

Real nanoparticle dispersions are never entirely monodisperse and can be substantially polydisperse. This calls for studying distributions of diffusion coefficients (or equivalently, distributions of sizes) and in conjunction with that, also distributions of concentration. In applications similar to those mentioned in the previous section, e.g. drug delivery and diagnostic markers, combining concentration measurements with estimation of size distributions strengthens the applicability of single particle fluorescence microscopy. For a particle with true diffusion coefficient D, the maximum likelihood estimate of D for a trajectory of k 2-dimensional positions $\mathbf{r}_1, ..., \mathbf{r}_k$ is

$$\hat{D} = \frac{1}{4\Delta t(k-1)} \sum_{i=1}^{k-1} \|\mathbf{r}_{i+1} - \mathbf{r}_i\|^2. \tag{1.13}$$

The distribution of $\hat{D}$ is a gamma distribution with parameters $k-1$ and $D/(k-1)$ and probability density

$$f_{\hat{D}|D,k}(x; D, k) = f_\Gamma\left(x; k-1, \frac{D}{k-1}\right) = \frac{(k-1)^{k-1}}{D^{k-1}\Gamma(k-1)} x^{k-2} e^{\frac{(k-1)x}{D}} \tag{1.14}$$

where $x \geq 0$ (see Braeckmans et al. (2010a) for more details).

Given that the true diffusion coefficients of a particle sample follow a probability distribution (density) f_D, the density $f_{\hat{D}}$ of diffusion coefficient estimates is

$$f_{\hat{D}}(x) = \int_0^\infty f_D(u) f_{\hat{D}|D}(x; u) du \tag{1.15}$$

where $f_{\hat{D}|D}$ is the probability density of diffusion coefficient estimates around a single true value D. Taking into account that the 'spread' around D depends on the trajectory length (a longer trajectory provides a more precise estimate

of D), this density can be written as a weighted sum of gamma densities,

$$f_{\hat{D}|D}(x;u) = \sum_{k=k_{\min}}^{\infty} \theta(u,k;k_{\min}) f_{\hat{D}|D,k}(x;u,k), \tag{1.16}$$

where $\theta(u,k;k_{\min})$ is the probability that a trajectory length is k, given that this length is larger than a cut-off $k_{\min}$ and that the true diffusion coefficient is u i.e.

$$\theta(u,k;k_{\min}) = P(K=k|K \geq k_{\min}, D=u), \tag{1.17}$$

c.f. Paper I. We assume similar to (Braeckmans et al., 2010a) that the true diffusion coefficients of the trajectories are distributed over a finite set of values $D_1, ..., D_I$. The distribution f_D of true diffusion coefficients becomes

$$f_D(x) = \sum_{i=1}^{I} \alpha_i \delta(x - D_i). \tag{1.18}$$

Here, α_i is the probability that the true diffusion coefficient of a (random) trajectory (of the particle responsible for a (random) trajectory) is D_i, and $\delta(\cdot)$ is the Dirac delta function. The model for the observed data, which are the diffusion coefficient estimates, now simplifies to

$$f_{\hat{D}}(x;\alpha) = \sum_{i=1}^{I} \alpha_i f_{\hat{D}|D}(x;D_i). \tag{1.19}$$

We use maximum likelihood (Pawitan, 2001) to estimate the parameters, with the log-likelihood function

$$l(\alpha) = \sum_{j=1}^{J} \log f_{\hat{D}}(\hat{D}_j;\alpha), \tag{1.20}$$

where $\hat{D}_j$, $j = 1, ..., J$, are the diffusion coefficient estimates from the trajectories and the distribution to be estimated is represented by $\alpha = (\alpha_1, ..., \alpha_I)$. Because of substantial "measurement error" i.e. large variance of the sampling distribution of the diffusion coefficient estimators, estimating the distribution of diffusion coefficients is a rather difficult problem. This is resolved by replacing the loglikelihood with a penalized loglikelihood (Silverman, 1982). A regularizing term of second derivatives (Good and Gaskins, 1971) is added to form the penalized loglikelihood. Regularization is not performed on the "level" of the diffusion coefficient estimates (the data) but rather on the "level" of the true diffusion coefficients. Henceforth, it is difficult to select the optimal value of ρ using e.g. cross-validation. Instead, we use what Terrell (1990) calls the

"maximum smoothing principle"; to select the maximum regularization consistent with the scale of the data as measured by e.g. a number of moments of the distribution. The α vector is first estimated using an initial guess for the axial size parameter. Subsequently, the axial size parameter is itself estimated. This process is repeated iteratively. In this fashion, both the distribution of diffusion coefficients and the (total) concentration are estimated simultaneously, see Fig. 1.5 for an example.

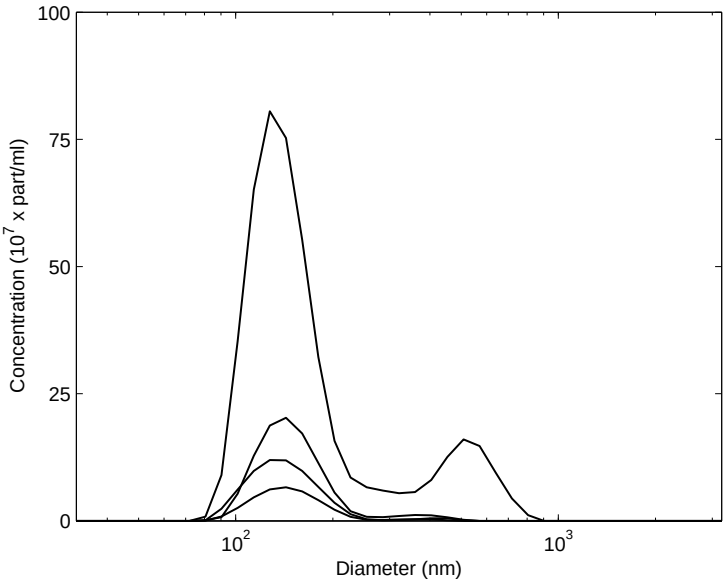

Figure 1.5: Estimated concentration distributions (as a function of particle size) of C16 PEG-Ceramide liposomes in whole blood as measured by fSPT 5, 20, 40, and 60 min (in order of decreasing total concentration) after intravenous injection into rats.

Chapter 2

Summary of papers

Four papers are included in this thesis. The first three papers cover stochastic modeling and statistical inference for absolute concentration measurements of monodisperse and polydisperse Brownian particles. The fourth paper covers a method for automated particle detection based on an analysis of time series correlations. In this chapter, brief summaries of these papers are given.

Paper I: Measuring absolute number concentrations of nanoparticles using single-particle tracking

In the first paper, we introduce a novel concept for estimation of the absolute particle number concentration in monodisperse Brownian particle dispersions using single particle tracking based on a model for the trajectory length (duration) distribution of particles. Inference in this model from experimental data of observed fluorescent carboxylated polymer nanospheres in water, of different diffusion coefficients (sizes) and concentrations, provides the means to estimate the size of the detection region where particles can be detected and tracked. Since this size depends on e.g. particle brightness and image processing settings, it would otherwise need to be estimated in a separate calibration measurement. A concentration estimate follows in a straightforward manner by relating the average number of detected particles by the size of the detection region. Excellent agreement is found between the theoretically and the experimentally obtained concentration values.

Paper II: Measuring absolute nanoparticle number concentrations from particle counts

The second paper introduces an alternative method to that of Paper I, also for monodisperse particles. The method uses a fluctuating time series of particle counts, known as a Smoluchowski process, to estimate absolute number concentrations in nanoparticle dispersions. Therefore, particle tracking is not required and detection of single particle positions is sufficient for the analysis. The downside is that the diffusion coefficient of the particles must be estimated separately. As in Paper I, the key step is estimation of the size of the detection region where particles can be detected, and from there the concentration estimate follows trivially. The method was validated experimentally by estimating the concentration of fluorescent carboxylated polymer nanospheres of different sizes and dilutions. A very good agreement between the concentration estimates and the reference measurements was found.

Paper III: Self-calibrated concentration measurements of polydisperse nano-particles

The third paper is a generalization of Paper I, where a distribution of diffusion coefficients (polydispersity) is assumed. The method enables size and absolute concentration measurements of polydisperse nanoparticles in solution based on single particle tracking. The method combines the method of Paper I with a method for estimation of a distribution of diffusion coefficients, enabling conversion of a probability distribution to a distribution of absolute concentration, accounting for some inherent statistical intricacies due to the somewhat peculiar sampling. Validation of the method is performed using simulations and experimental data of polystyrene nanospheres. As an application of the method, aggregation and clearance of different types of liposomal drug carriers is studied after intravenous injection in rats.

Paper IV: Automatic particle detection in microscopy using temporal correlations

The fourth paper is independent of the other three, although a result of the analysis behind Paper II. The method proposed in the paper concerns the de-

tection of particles in microscope images. Typically, a plausible set of particles is obtained from a larger set of candidate particles by filtering using threshold values for intensity, size, shape, and other parameters that are manually selected. By analysis of the correlation structure of a time series of particle counts, known as a Smoluchowski process, and the impact of false negatives and false positives, an optimality criterion for automatic threshold selection is found. Three experimental data sets are used to evaluate the performance by comparing manually selected threshold values from three independent experts with the automatically selected threshold values. The method shows promise and produces useful results, thus reducing the need for manual intervention in image analysis for single particle microscopy.

Chapter 3

Outlook

In Paper I, the most obvious problem is the approximation of a 3-dimensional system with a 1-dimensional model. Numerical computations involved in calculating the trajectory length distribution is tremendously simplified by this approximation, but the downside is the introduction of an asymptotic bias. Studies (not shown) have indicated that using simulation-based inference, e.g. simulated method of moments can reduce computation time by an order of magnitude even including an extension to 3 dimensions. Approximate Bayesian computation (ABC) would also be an interesting approach for this problem. Thereby, asymptotic bias can be removed in the estimation of the axial size of the detection region. The downside here is the additional variance induced by the stochastic nature of the inference scheme.

In Paper II, it is easily shown that the Smoluchowski process is not Markov, since the correlation structure of the process is not a geometrically decreasing function of the time lag. However, the transition probabilities derived are 'marginally' true, i.e. the expression for $P(X_k = x_k|X_{k-1} = x_{k-1})$ is exact for any k, but the full likelihood still underestimates correlations on longer scales than Δt because of the Markov assumption. This suggests that the estimator may be consistent and it would be interesting to provide a proof. It is also interesting to consider possible implications of this modeling to the modeling in Paper I. The Smoluchowski process can be thought of as a discrete-time M/G/∞ queue with G being non-geometric (but with a geometric tail) and being equal to the trajectory length distribution. It is not likely that this would lead to a simplified expression for G, but if the expected value of G could be derived, the method of moments could be used for improving the results of Paper I the result would be both a massive reduction in computational time and

the removal of asymptotic bias. Another interesting topic is how to perform simultaneous estimation of diffusion coefficient and detection region size in this setting. It is likely that by considering subregions of the detection region, i.e. forming a vector-valued Smoluchowski process, this can be resolved, although it is not obvious what the consequences would be for inference.

In Paper III, the model for the distribution of diffusion coefficients is discrete. Introduction of a continuous model would be appealing. A mixture of inverse gamma distributions would give an analytically tractable likelihood (not shown). However, since the bias correction is by necessity performed in a discrete setting, the current implementation was more consistent. Constructing an alternative model by considering individual particle positions and increments instead of trajectories could remove the need for a bias correction, possibly thereby opening for a completely continuous model.

In Paper IV, it would be of much interest to understand the particular circumstances under which the maximization of the correlation criterion is sensible. The most general, i.e. unconstrained, form of correlation maximization would mean the inclusion or exclusion of each particle position on an individual basis, without reference to its properties such as size or intensity, thus having a parameter space with as many dimensions as there are particle positions. This is clearly not physically plausible, since the selection of particles would be inconsistent. The other extreme is to reduce the problem to the global selection of a single parameter threshold for, say, size, which is too narrow a condition. A key issue is to determine under what constraints the principle can be used to produce plausible results, and what image analysis workflows can be used in conjunction with this method. Also, it is of some interest to incorporate the possibility to make corrections by including or excluding particles by manually specifying constraints for subregions of an image.

Bibliography

Apgar, J., Tseng, Y., Fedorov, E., Herwig, M., Almo, S., and Wirtz, D. (2000). Multiple-particle tracking measurements of heterogeneities in solutions of actin filaments and actin bundles. *Biophysical Journal*, 79:1095–1106.

Bausch, A. and Weitz, D. (2002). Tracking the dynamics of single quantum dots: Beating the optical resolution twice. *Journal of Nanoparticle Research*, 4:477–481.

Berg, H. C. (1993). *Random Walks in Biology*. Princeton University Press.

Bornfleth, H., Satzler, H., Eils, R., and Cremer, C. (1998). High-precision distance measurements and volume-conserving segmentation of objects near and below the resolution limit in three-dimensional confocal fluorescence microscopy. *Journal of Microscopy*, 189:118–136.

Braeckmans, K., Buyens, K., Bouquet, W., Vervaet, C., Joye, P., de Vos, F., Plawinski, L., Doeuvre, L., Anglés-Cano, E., Sanders, N., Demeester, J., and de Smedt, S. (2010a). Sizing nanomatter in biological fluids by fluorescence single particle tracking. *Nano Letters*, 10:4435–Ũ4442.

Braeckmans, K., Vercauteren, D., Demeester, J., and de Smedt, S. (2010b). Single particle tracking. In Diaspro, E., editor, *Nanoscopy multidimensional optical fluorescence microscopy*. Taylor and Francis.

Carter, B., Shubeita, G., and Gross, S. (2005). Tracking single particles: a user-friendly quantitative evaluation. *Physical Biology*, 2:60–72.

Chandrasekhar, S. (1943). Stochastic problems in physics and astronomy. *Reviews of Modern Physics*, 15(1):1–89.

Cheezum, M., Walker, W., and Guilford, W. (2001). Quantitative comparison of algorithms for tracking single flourescent particles. *Biophysical Journal*, 81:2378–2388.

Chironi, G., Boulanger, C., Simon, A., Dignat-George, F., Freyssinet, J., and Tedgui, A. (2009). Endothelial microparticles in diseases. *Cell and Tissue Research*, 335:143–151.

Crocker, J. and Grier, D. (1996). Methods of digital video microscopy for colloidal studies. *Journal of Colloid and Interface Science*, 179:298–310.

Daley, D. and Vere-Jones, D. (2003). *An introduction to the theory of point processes. Volume I: Elementary theory and methods*. Springer.

Decuzzi, P., Godin, B., Tanaka, T., Lee, S.-Y., Chiappini, C., Liu, X., and Ferrari, M. (2010). Size and shape effects in the biodistribution of intravascularly injected particles. *Journal of Controlled Release*, 141:320–327.

Delehanty, J., Mattoussi, H., and Medintz, I. (2009). Delivering quantum dots into cells: strategies, progress and remaining issues. *Analytical and Bioanalytical Chemistry*, 393:1091–105.

Deniz, A., Mukhopadhyay, S., and Lemke, E. (2008). Single-molecule biophysics: at the interface of biology, physics and chemistry. *Journal of the Royal Society Interface*, 5:15–45.

Deschout, H., Neyts, K., and Braeckmans, K. (2012). The influence of movement on the localization precision of sub-resolution particles in fluorescence microscopy. *Journal of Biophotonics*, 5:97–109.

Doevre, L., Plawinski, L., Toti, F., and Anglés-Cano, E. (2009). Cell-derived microparticles: a new challenge in neuroscience. *Journal of Neurochemistry*, 110:457–468.

Doob, J. (1953). *Stochastic processes*. Wiley.

Dragovic, R., Gardiner, C., Brooks, A., Tannetta, D., Hole, D. F. P., Carr, B., Redman, C., Harris, A., Dobson, P., Harrison, P., and Sargent, I. (2011). Sizing and phenotyping of cellular vesicles using Nanoparticle Tracking Analysis. *Nanomedicine*, 7:780–788.

Du, S., Kendall, K., Morris, S., and Sweet, C. (2010). Measuring number-concentrations of nanoparticles and viruses in liquids on-line. *Journal of Chemical Technology and Biotechnology*, 85:1223Ű–1228.

Einstein, A. (1905). Über die von der molekulärkinetischen Theorie der Wärme gefordete Bewegung von in ruhenden Flüssigkeiten suspendierten Teilchen (On the movement of small particles suspended in stationary liquids required by the molecular-kinetic theory of heat). *Annalen der Physik*, 17:549–560.

Filipe, V., Poole, R., Kutscher, M., Forier, K., Braeckmans, K., and Jiskoot, W. (2012a). Fluorescence single particle tracking for the characterization of submicron protein aggregates in biological fluids and complex formulations. *Pharmaceutical Research*, 28:1112–1120.

Filipe, V., Poole, R., Kutscher, M., Forier, K., Braeckmans, K., and Jiskoot, W. (2012b). Monitoring subvisible aggregates of monoclonal IgG in serum. *Pharmaceutical Research*, 29:2202–2212.

Frangioni, J. (2006). Self-illuminating quantum dots light the way. *Nature Biotechnology*, 24:326–328.

Gaumet, M., Vargas, A., Gurny, R., and Delie, F. (2008). Nanoparticles for drug delivery: the need for precision in reporting particle size parameters. *European Journal of Pharmaceutics and Biopharmaceutics*, 69:1–9.

Genovesio, A., Liedl, T., Emiliani, V., Parak, W., Coppey-Moisan, M., and Olivo-Marin, J.-C. (2006). Multiple particle tracking in 3-d+ microscopy: Method and application to the tracking of endocytosed quantum dots. *IEEE Transactions on Image Processing*, 15:1062–1070.

Good, I. J. and Gaskins, R. A. (1971). Nonparametric roughness penalties for probability densities. *Biometrika*, 58:255–277.

Holtzer, L. and Schmidt, T. (2010). The tracking of individual molecules in cells and tissues. In Brächle, C., Lamb, D., and Michaelis, J., editors, *Single particle tracking and single molecule energy transfer*. Wiley.

Hong, G., Lee, J., Robinson, J., Raaz, U., Xie, L., Huang, N., Cooke, J., and Dai, H. (2012). Multifunctional in vivo vascular imaging using near-infrared ii fluorescence. *Nature Medicine*, 18:1841–1846.

Jaqaman, K., Loerke, D., Mettlen, M., Kuwata, H., Grinstein, S., Schmid, S., and Danuser, G. (2008). Robust single-particle tracking in live-cell time-lapse sequences. *Nature Methods*, 5:695–702.

Kelley, A., Michalet, X., and Weiss, S. (2001). Chemical physics. Single-molecule microscopy comes of age. *Science*, 292:1671–1672.

Khare, S. and Dokholyan, N. (2007). Molecular mechanisms of polypeptide aggregation in human diseases. *Current Protein and Peptide Science*, 8:573–579.

Koide, H., Asai, T., Urakami, K. H. T., Ishii, T., Kenjo, E., Nishihara, M., Yokoyama, M., Ishida, T., Kiwada, H., and Oku, N. (2008). Particle size-dependent triggering of accelerated blood clearance phenomenon. *International Journal of Pharmaceutics*, 362:197–200.

Levi, V. and Gratton, E. (2010). Three-dimensional particle tracking in a laser scanning fluorescence microscope. In Brächle, C., Lamb, D., and Michaelis, J., editors, *Single particle tracking and single molecule energy transfer*. Wiley.

Lim, Y., Kim, S., Nakayama, A., Stott, N., Bawendi, M., and Frangioni, J. (2003). Selection of quantum dot wavelengths for biomedical assays and imaging. *Molecular Imaging*, 2:50–64.

Lundqvist, M., Stigler, J., Elia, G., Lynch, I., Cedervall, T., and Dawson, K. (2008). Nanoparticle size and surface properties determine the protein corona with possible implications for biological impacts. *Proceedings of the National Academy of Sciences*, 105:14265–14270.

McDonald, D., Vodicka, M., Lucero, G., Svitkina, T., and Borisy, G. (2002). Visualization of the intracellular behavior of HIV in living cells. *Journal of Cell Biology*, 159:441–452.

Meijering, E., Dzyubachyk, O., Smal, I., and van Cappellen, W. (2009). Tracking in cell and developmental biology. *Seminars in Cell and Developmental Biology*, 20:894–902.

Michalet, X., Pinaud, F., Bentolila, L., Tsay, J., Doose, S., Li, J., Sundaresan, G., Wu, A., Gambhir, S., and Weiss, S. (2005). Quantum dots for live cells, in vivo imaging, and diagnostics. *Science*, 307:538–544.

Montes-Burgos, I., Walczyk, D., Hole, P., Smith, J., Lynch, I., and Dawson, K. (2010). Characterisation of nanoparticle size and state prior to nanotoxicological studies. *Journal of Nanoparticle Research*, 12:47–53.

Morris, A., Watzky, M., and Finke, R. (2009). Protein aggregation kinetics, mechanism, and curve-fitting: A review of the literature. *Biochimica et Biophysica Acta*, 1794:375–397.

Mortensen, K., Churchman, L., Spudich, J., and Flyvbjerg, H. (2010). Optimized localization analysis for single-molecule tracking and super-resolution microscopy. *Nature Methods*, 7:377–381.

Nel, A., Mädler, L., Velegol, D., Xia, T., Hoek, E., Somasundaran, P., Klaessig, F., Castranova, V., and Thompson, M. (2009). Understanding biophysicochemical interactions at the nano-bio interface. *Nature Materials*, 8:543–557.

Nune, S., Gunda, P., Thallapally, P., Lin, Y., Forrest, M., and Berkland, C. (2009). Nanoparticles for biomedical imaging. *Expert Opinion on Drug Delivery*, 6:1175–1194.

Ober, R., Ram, S., and Ward, E. (2004). Localization accuracy in single-molecule microscopy. *Biophysical Journal*, 86:1185–1200.

Pawitan, Y. (2001). *In All Likelihood: Statistical Modelling and Inference Using Likelihood*. Oxford University Press, Oxford, UK.

Remaut, K., Sanders, N., de Geest, B., Braeckmans, K., Demeester, J., and de Smedt, S. (2007). Nucleic acid delivery: Where material sciences and bio-sciences meet. *Materials Science and Engineering: R*, 58:117Ű–161.

Röding, M. (2011). *Concentration measurements in single particle microscopy*. Licentiate thesis, Chalmers University of Technology.

Sage, D., Neumann, F., Hediger, F., Gasser, S., and Unser, M. (2005). Automatic tracking of individual fluorescence particles: Application to the study of chromosome dynamics. *IEEE Transactions on Image Processing*, 14:1372–1383.

Saxton, M. (2009). Single-particle tracking. In Jue, T., editor, *Fundamental concepts in biophysics*. Springer.

Saxton, M. and Jacobson, K. (1997). Single-particle tracking: Applications to membrane dynamics. *Annual Review of Biophysics and Biomolecular Structure*, 26:373–399.

Silverman, B. (1982). On the estimation of a probability density function by the maximum penalized likelihood method. *Annals of Statistics*, 10(3):795–810.

Smal, I., Draegestein, K., Galjart, N., Niessen, W., and Meijering, E. (2008). Particle filtering for multiple object tracking in dynamic fluorescence microscopy images: Application to microtubule growth analysis. *IEEE Transactions on Medical Imaging*, 27:789–804.

Smal, I., Loog, M., Niessen, W., and Meijering, E. (2010). Quantitative comparison of spot detection methods in fluorescence microscopy. *IEEE Transactions on Medical Imaging*, 29:282–301.

Soenen, S., Vercauteren, D., Braeckmans, K., Noppe, W., Smedt, S. D., and Cuyper, M. D. (2009). Stable long-term intracellular labelling with fluorescently tagged cationic magnetoliposomes. *ChemBioChem*, 10:257–267.

Svedberg, T. and Inouye, K. (1911). Eine neue Methode zur Prüfung der Gültigkeit des Boyle-Gay-Lussacschen Gesetzes für kolloide Lösungen (A novel method of proving the validity of the Boyle-Gay-Lussac law for colloidal dispersions). *Zeitschrift für Physikalische Chemie*, 77:145–190.

Terrell, G. (1990). The maximal smoothing principle in density estimation. *Journal of the American Statistical Association*, 85:470–477.

Thomann, D., Rines, D., Sorger, P., and Danuser, G. (2002). Automatic fluorescent tag detection in 3d with super-resolution: Application to the analysis of chromosome movement. *Journal of Microscopy*, 208:49–64.

Thompson, R., Larson, D., and Webb, W. (2002). Precise nanometer localization analysis for individual fluorescent probes. *Biophysical Journal*, 82:2775–2783.

Toomre, D., Keller, P., White, J., Olivo-Marin, J.-C., and Simons, K. (1999). Dual-color visualization of trans-golgi network to plasma membrane traffic along microtubules in living cells. *Journal of Cell Science*, 112:21–33.

van Gaal, E., Spierenburg, G., Hennink, W., Crommelin, D., and Mastrobattista, E. (2009). Flow cytometry for rapid size determination and sorting of nucleic acid containing nanoparticles in biological fluids. *Journal of Controlled Release*, 141:328–338.

van Gaal, E., Spierenburg, G., Hennink, W., Crommelin, D., and Mastrobattista, E. (2010). Flow cytometry for rapid size determination and sorting of nucleic acid containing nanoparticles in biological fluids. *Journal of Controlled Release*, 141:328–338.

von Smoluchowski, M. (1906). Zur kinetischen Theorie der Brownschen Molekularbewegung und der Suspensionen (On the kinetic theory of Brownian molecular motion and suspensions). *Annalen der Physik*, 21:756–780.

von Smoluchowski, M. (1916). Drei Vorträge über Diffusion, Brownsche Molekularbewegung und Koagulation von Kolloidteilchen (Three lectures on diffusion, Brownian molecular motion and coagulation of colloidal particles). *Physikalische Zeitschrift*, 17:557–571 and 587–599.

Vysotskii, V., Uryupina, O., Guselńikova, A., and Roldugin, V. (2009). On the feasibility of determining nanoparticle concentration by the dynamic light scattering method. *Colloid Journal*, 71:739–Ű744.

Walter, N., Huang, C.-Y., Manzo, A., and Sobhy, M. (2008). Do-it-yourself guide: how to use the modern single-molecule toolkit. *Nature Methods*, 5:475–489.

Welsher, K., Liu, Z., Sherlock, S., Robinson, J., Chen, Z., Daranciang, D., and Dai, H. (2009). A route to brightly fluorescent carbon nanotubes for near-infrared imaging in mice. *Nature Nanotechnology*, 4:773–780.

Westgren, A. (1916). Die Veränderungsgeschwindigkeit der lokalen Teilchenkonzentration in kolloiden Systemen, I. (The change velocity of the local particle concentration in colloidal systems). *Arkiv för Matematik, Astronomi och Fysik*, 11:1–24.

Yildiz, A. and Selvin, P. (2004). Kinesin walks hand-over-hand. *Science*, 303:676–678.

Zimmer, C., Labruyere, E., Meas-Yedid, V., Guillen, N., and Olivo-Marin, J.-C. (2002). Segmentation and tracking of migrating cells in videomicroscopy with parametric active contours: a tool for cell-based drug testing. *IEEE Transcations on Medical Imaging*, 21:1212–1221.

Zlatanova, J. and van Holde, K. (2006). Single-molecule biology: what is it and how does it work? *Molecular Cell*, 24:317–329.